Electronic Supplementary Information (ESI) Document

Solvent Based Dissolution-Precipitation of Waste Polyethylene Terephthalate: Economic and Environmental Performance Metrics

Utkarsh S. Chaudhari [a, *], Daniel G. Kulas [a], Alejandra Peralta [b], Tasmin Hossain [c], Anne T. Johnson [d], Damon S. Hartley [c], Robert M. Handler [a], Barbara K. Reck [e], Vicki S. Thompson [f], David W. Watkins [g], David R. Shonnard [a]

[a] Department of Chemical Engineering, Michigan Technological University, Houghton, Michigan 49931, USA.

[b] Chemstations Inc., Houston, Texas 77042, USA.

[c] Operations Research and Analysis, Idaho National Laboratory, Idaho Falls, Idaho 83415, USA

[d] Resource Recycling Systems, Ann Arbor, Michigan 48105, USA.

[e] Center for Industrial Ecology, Yale School of the Environment, New Haven, Connecticut 06511, USA.

[f] Biological & Chemical Science & Engineering Department, Idaho National Laboratory, Idaho Falls, Idaho 83415, USA.

[g] Department of Civil, Environmental, and Geospatial Engineering, Michigan Technological University, Houghton, Michigan 49931, USA.

[*] Corresponding Author: uschaudh@mtu.edu. Phone No. +1 906 370 8392

No. of Figures: 9

No. of Tables: 11

Section 1. Review of Economic and Environmental Studies

Evolving chemical recycling technologies can be broadly classified into three main categories that mainly differ based on the product(s) obtained from these processes [1]. They are classified as: 1: Purification (also referred as Dissolution / Solvent-based recycling / Dissolution-Precipitation / Solvent Targeted Recovery And Precipitation (STRAP); "Plastic-to-Plastic"), 2. Depolymerization (sometimes referred as solvolysis [2]; "Plastics-to-monomers"), 3. Conversion recycling technologies ("Plastics-to-intermediate hydrocarbon products" such as naphtha for cracking to new plastics, specialty chemicals, waxes, lubricants, fuels, and gases).

Table S1 shown below summarizes our literature review of technoeconomic analysis (TEA) and life cycle assessment (LCA) studies on chemical recycling technologies. We found that most of these studies are focused on the conversion recycling technologies ("plastics-to-intermediate hydrocarbon products") such as pyrolysis, gasification etc. Among the depolymerization technologies, enzymatic depolymerization was the most studied, followed by methanolysis, alkaline hydrolysis, and glycolysis. Some of the other studies looked at dissolution of post-industrial multi-layer PET based film using non-green solvents and recovery of polymer(s) by two methods: first, addition of anti-solvent to the polymer solution; and second, reducing the temperature of polymer solution [3-5]. Another study looked at dissolution of PET using non-green solvent and precipitation via anti-solvent approach [6]. Apart from our previous study [7], no TEA and LCA studies were found on dissolution of waste PET using a green solvent and precipitation via evaporation.

Table S1. Literature review on technoeconomic and life cycle assessment studies on chemical recycling technologies.

No.	Reference	Technology	Year	LCA	TEA	Process simulation	Type of plastic processed
1	[8]	Pyrolysis	2019	-	✓	✓	HDPE
2	[9]	Pyrolysis	2019	✓	-	✓	HDPE
3	[10]	Liquid fed pyrolysis	2022	✓	✓	✓	HDPE/PP
4	[11]	Pyrolysis and Gasification	2020	✓	✓	✓	PP

5	12	Pyrolysis	2023	✓	✓	✓	Mixed plastic waste
6	13	Pyrolysis	2020	-	✓	✓	Mixed plastic waste
7	14	Pyrolysis	2022	-	✓	✓	HDPE
8	15	Pyrolysis	2022	-	✓	-	Mixed plastic waste (HDPE, LDPE, PP, PS)
9	16	Pyrolysis	2017	✓	-	-	HDPE, LDPE, PP
10	17	Pyrolysis	2018	-	✓	✓	PE, PP, PS
11	18	Pyrolysis	2020	-	✓	-	Mixed plastic waste
12	19	Pyrolysis	2021	-	✓	-	Mixed plastic waste
13	20	Pyrolysis	2021	✓	-	-	Mixed plastic waste
14	21	Pyrolysis	2022	✓	-	-	HDPE (25 wt%), LDPE (33 wt%) and PP (42 wt%)
15	22	Pyrolysis	2022	✓	-	-	HDPE and High impact polystyrene (HIPS)
16	23	Gasification	2023	-	✓	✓	Mixed plastic waste

17	[24]	Gasification	2022	✓	✓	-	Mixed plastic waste
18	[25]	Gasification	2022	✓	✓	✓	Mixed plastic waste
19	[26]	Pyrolysis, Gasification, Dissolution (Anti-solvent), Depolymerization (Glycolysis; Hydrolysis)	2021	✓	-	-	25 polymers
20	[27]	Gasification	2022	✓	-	-	Mixed plastic waste
21	[28]	Hydrogenolysis	2022	✓	✓	✓	HDPE
22	[29]	Hydrothermal Treatment	2023	✓	-	-	PP and PE films and flexible plastics
23	[30]	Gasification and Pyrolysis	2022	✓	-	-	MSW
24	[31]	Gasification	2022	✓	✓	-	Mixed plastics
25	[32]	Gasification	2022	✓	✓	-	Mixed plastics
26	[33]	Gasification	2023	-	✓	✓	PE and PET
27	[5]	Dissolution (Anti-solvent; Cooling)	2020	-	✓	✓	Multilayer PET based post-industrial film

28	4	Dissolution (Anti-solvent; Cooling)	2021	-	✓	✓	Multilayer PET based post-industrial film
29	3	Dissolution (Anti-solvent; Cooling)	2022	✓	-	✓	Multilayer PET based post-industrial film
30	34	Dissolution (Anti-solvent)	2019	-	✓	✓	LDPE
31	35	Dissolution	2023	✓	-	-	Polyester/ elastane and polyamide/ elastane blends
32	36	Enzymatic depolymerization	2021	✓	✓	✓	PET
33	37	Enzymatic depolymerization	2021	-	✓	✓	PET
34	38	Depolymerization (Alkaline hydrolysis)	2021	✓	-	-	PET
35	39	Enzymatic depolymerization	2022	✓	-	✓	PET
36	40	Depolymerization (Alkaline hydrolysis)	2020	✓	-	✓	PET
37	6	Pyrolysis, Gasification, Depolymerization (Glycolysis; Methanolysis; Enzymatic), Dissolution (Anti-solvent)	2023	✓	✓	✓	PET and polyolefin plastics
38	41	Depolymerization (Methanolysis; Enzymatic)	2023	✓	-	-	PET

39	42	Pyrolysis	2022	✓	✓	-	Waste surgical masks (PP and non-woven fabrics)
40	43	Pyrolysis	2022	✓	✓	✓	Personal protective equipment (PPE)
41	44	Pyrolysis	2021	✓	✓	✓	HDPE
42	45	Pyrolysis, Gasification, Hydrocracking, Hydrothermal liquefaction, Hydrogenolysis	2023	✓	✓	✓	LDPE
43	46	Dissolution (Cooling)	2023	✓	✓	✓	PP based masks
44	47	Dissolution (Cooling)	2023	✓	✓	✓	Multi-layer post-industrial film

Section 2. Technoeconomic Analysis

Table S2 provides a summary of assumptions used in our TEA along with pricing data for raw materials and products [48]. More information on estimation of economic performance metrics is shown after Table S2.

Table S2. Technoeconomic parameters and assumptions used for economic analysis of waste PET dissolution processes.

Parameter	Value
Lifetime of Plant (Years)	30
Operating Days (Days/year)	350
Total CR-PET produced (MT/year)	8400
Base year	2019
OSBL Costs	100% of ISBL
Engineering Costs	25% of ISBL + OSBL costs
Contingency Costs	10% of ISBL + OSBL costs
Working Capital	5% of FCI
Depreciation Method & recovery period	7-year MACRS

Construction period (Years) and spending schedule [49]	3 Years (8% Y1, 60% Y2, 32% Y3)
Start-up time (Years)	0.5
Income tax rate (%)	21%
Internal rate of return (IRR) (%)	20%
Supervision	25% of operating labor
Direct overhead	50% of operating labor and supervision
General & administrative costs (G&A costs)	65% of total labor costs
Maintenance costs	5% of ISBL costs
Insurance costs	1% of ISBL+OSBL costs
Baled PET price (10-year average, $/MT) [50]	377
Bale pretreatment Cost ($/MT)	100
R-PET price (10-year average, $/MT) [50]	1,608
GVL price ($/MT) [51]	1,000
Waste disposal cost ($/MT, U.S. average) [52]	55
Electricity ($/kWh) [53]	0.0681
Cooling water ($/GJ) [54]	0.381
Natural gas ($/GJ) [55]	3.7
High, medium, and low-pressure steam ($/GJ) [54]	6.5, 3.54, and 2.76, respectively

Note: ISBL: Inside battery limit investment; OSBL: Outside/offsite battery limit investment; FCI: Fixed capital investment; MACRS: Modified Accelerated Cost Recovery System.

Net Present Value

The net present value (NPV) is a useful economic measure of the profitability of a process and represents the annual sum of all the present values of the future cash flows, given by the following equation (eq.) S1:

$$NPV = \sum_{n=1}^{n=t} \frac{Cash\ flow_n}{(1+i)^n} \qquad \textbf{Eq. S1}$$

Where, ‘n’ represents the year, ‘t’ represents the lifetime of the plant, and ‘i’ represents the internal rate of return. A project with higher NPV is desired representing higher profitability [48]. An NPV = 0 means that the project just achieves the established profitability targets, so a positive NPV provides additional confidence in the viability of the project.

Minimum Selling Price

The minimum selling price (MSP) of a product is found by setting the NPV = 0 by changing the initial selling price of the product and represents the minimum required price of the product at which it should be sold at for the process to break even at the end of project and achieve the expected internal rate of return.

Discounted Internal Rate of Return

The discounted internal rate of return is found by setting the NPV = 0 by varying initially assumed internal rate of return (20%, see Table S2) at an assumed selling price of the product ($1,608/MT, see Table S2). A project with higher NPV represents higher profitability and, therefore, would be able to offer a higher discounted internal rate of return. It is a more useful method than NPV to compare different project sizes [48].

Return on Investment

The return on investment (ROI) [48] was calculated an average over the whole project as shown in eq. S2:

$$ROI\ (\%) = \frac{Cumulative\ net\ profit}{plant\ life\ \times initial\ investment} \times 100 \qquad \textbf{Eq. S2}$$

Payback Period

A simple payback period (after tax) [48] was calculated as shown in the eq. S3:

$$Payback\ period\ (Years) = \frac{Total\ investment}{Average\ annual\ cash\ flow} \qquad \textbf{Eq. S3}$$

Section 3. PET Bale Transportation Model

A simple model for transporting bales was developed based on methods in the literature [56, 57]. This model was initially developed for biomass material and biorefineries, but we modified this same model for its application to end-of-life plastic materials and chemical recycling. This model was also integrated with the TEA and LCA to evaluate transportation cost and environmental impacts as a function of facility capacity, and therefore bale transport distance. To build this simple transportation model, the following assumptions were made: 1) Chemical recycling facility to be located in the EPA region 5, that would source its feedstock from the Illinois, Indiana, Michigan, Minnesota, Ohio, and Wisconsin; 2) Single mode of transportation via a combination truck; 3) Non-fiber PET packaging waste was uniformly distributed around the chemical recycling facility in a circular area; 4) All of the non-fiber PET packaging waste that is generated per capita was collected for sorting and recycling.

For a centrally located chemical recycling facility, the average one-way delivery distance (miles) to the facility could be calculated as shown in eq. S4 below:

$$r^{Average}_{Circle} = \left(\frac{2}{3}\tau\sqrt{\frac{C}{\pi\, Y\, f}}\right) \times 0.0395 \qquad \textbf{Eq. S4}$$

where,

τ : Winding factor (also called as tortuosity factor)
C : Total plastic waste to be collected or required for facility in MT/year (capacity)
Y : Amount of non-fiber PET waste available in MT/Acre
f : Fraction of urban land surrounding the facility (0.054)

The value ‘0.0395’ in the eq. S4 is the unit conversion factor for square root of acres to miles. For the base capacity, the average one-way delivery distance was found to be 33 miles (54 km).

The winding factor, τ, could range anywhere between 1.2 to 3.0 and is required to account for the irregularities in the road network that depends on the regional development and nature of the road infrastructure [56, 58]. It is defined as the ratio of the actual distance traveled by a truck to the straight-line distance to the facility [56]. In our work, it was assumed to be 1.2 based on Hossain et al. [59]. The total amount of plastic waste collected for chemical recycling, C (MT/year), also includes the presence of contaminants in the feedstock, which was assumed to be 10%, as well as the polymer loss of 1% during the solvent based dissolution process, as mentioned in the methods section. For the base capacity, the value of C was 9,438 MT/year. The total amount of non-fiber PET packaging waste available in EPA region 5, in metric tons, was determined by multiplying the total population of EPA region 5 (53.1 million people[60]) by the national non-fiber PET packaging waste generated (3.502 MT[61]) per capita (331.5 million people[60]; 0.011 MT/capita). This was then divided by the total urban land area of EPA region 5 yielding 0.051 MT of non-fiber PET packaging waste generated per acre, Y. The formula for calculating Y is shown below in eq. S5:

$$Y = \frac{\left(\frac{National\ PET\ waste\ generated}{Total\ U.S.\ Population}\right) \times Total\ population\ of\ EPA\ R5}{Total\ Urban\ Land\ Area\ of\ EPA\ R5} \quad \textbf{Eq. S5}$$

The fraction of urban land surrounding the facility, *f*, was determined by taking the ratio of total urban land area in EPA region 5 (11,051,413 acres[62]) to the total land area in EPA region 5 (206,464,006 acres[62]). The urban area was considered because 80% of the total U.S. population resides in the urban areas [63]. Also, it was assumed that any of the waste collected in the rural area would be transported to the MRF located in the urban areas. The formula for the *f* factor is shown below in eq. S6:

$$f = \frac{Total\ Urban\ Land\ Area\ of\ EPA\ R5\ in\ Acre}{Total\ Land\ Area\ of\ EPA\ R5\ in\ Acre} \quad \textbf{Eq. S6}$$

While the eq. S4 tells us the average one-way delivery distance, the maximum distance around the facility from which the feedstock must be collected is shown by eq. S7 and was adopted from [56]:

$$r_{Circle}^{Max.} = \sqrt{\frac{C}{\pi\, Y\, f}} \quad \textbf{Eq. S7}$$

The average transportation costs, including roundtrip distance (factor of 2 in eq S8), could be calculated using eq. S8:

$$Total\ Avg.\ Transportation\ Costs\left(\frac{\$}{Year}\right) = 2 \times r_{Circle}^{Average}(miles) \times Unit\ Delivery\ Cost\left(\frac{\$}{MT - miles}\right) \times C \quad \textbf{Eq. S8}$$

The unit delivery cost for hauling plastic bales, in $/MT-miles, was obtained from colleagues at Idaho National Laboratory, which includes fixed as well as variable operating costs for transportation. For the base capacity, the unit delivery cost was $0.108/MT-miles.

The GHG emissions and cumulative energy demand (CED) associated with transportation were calculated by multiplying the amount of feedstock transported for an average one way distance travelled with the GHG emission (kg CO_2-eq/MT-km) and CED factor (MJ/MT-km) related to combination truck, as mentioned above in the first paragraph of this section. The GHG emission and CED factor for combination truck were 0.0956 kg CO_2-eq/MT-km and 1.28 MJ/MT-km, which were obtained from the SimaPro eco-invent 2.2 database (Eco-profile: Transport, combination truck, average fuel mix NREL/US U, Ecoinvent 2.2, Diesel powered).

Sample calculation for estimating transportation related GHG emissions for the base capacity (8,400 MT/year):

Average GHG emissions (kg CO_2-eq/kg of CR-PET) = 0.0956 kg CO_2-eq/MT-km * 0.00112 MT/kg of CR-PET * 54 km = 0.006

Note that the amount of material transported is based on the functional unit used for the LCA (see Table S3). Therefore, the only variable in the above calculation shown is the average one-way delivery distance (54 km, obtained from eq. S4), which will change with change in capacity. The average one-way delivery distance was chosen because the GHG emission and CED factor for transportation already accounts for the impacts of empty return trip[64, 65]. Increasing capacity demands more feedstock for the process, which would need to be sourced and transported over longer distances. Therefore, these impacts would increase with increase in the capacity. The CED impacts were calculated in a similar manner, as shown in the example above, but just with the CED factor.

Section 4. Life Cycle Assessment

Table S3. Life cycle input data for chemical recycling of PET via dissolution-precipitation technology. Inputs based on 1 kg of CR-PET produced.

Inputs	**Anti-solvent**		**Evaporation**		**Cooling**	**Unit**
	Base case	**HIX**	**Base case**	**HIX**		
Collection, sorting, and baling [a]	1.12					kg
PET flakes to dissolution [a]	1.01					kg
Gamma-Valerolactone (GVL) solvent [b]	0.06 (make-up for losses)					kg
Electricity, medium voltage {US, US only}| market for | APOS, U	0.081	0.081	0.093	0.093	0.118	MJ

Heat, from steam, in chemical industry {RER}| market for heat, from steam, in chemical industry | APOS, U	24.65	24.15	2.66	2.15	1.60	MJ
Heat, district or industrial, natural gas {RER}| market group for | APOS, S	1.3	1.3	0	0	0	MJ
Water, decarbonised {US}| market for water, decarbonised | APOS, S	204.47	200.43	18.64	14.60	10.22	kg
Process waste	0.182					kg

Notes: [a]: LCA impacts sourced from Franklin Associates report [66]; [b]: The eco-profile for GVL solvent was not found in the Ecoinvent database. Butyrolactone solvent (Butyrolactone {GLO}| market for | APOS, U) was used as a substitute for GVL based on their structural similarities and boiling points. This lack of LCA data for GVL solvent has also been recognized by other researchers [47].

Section 5. Results

Fig. S1 represents the overall material balance on the modeled processes to produce 1 MT/hour of chemically recycled PET (CR-PET). About 1.12 MT/hour of baled PET feedstock would be required to produce 1 MT/hour of CR-PET. A 10% loss of the incoming baled PET feedstock was assumed to be removed during the pretreatment step, as mentioned in the methods section. About 0.06 MT/hour of make-up GVL solvent was required for the process, which was lost during the filtration step in the process. The total process waste (0.07MT/hour) includes the polymer loss (0.01 MT/hour) and solvent loss (0.06 MT/hour). Material stream flows and compositions are shown in Table S4-S6 for each of the processes.

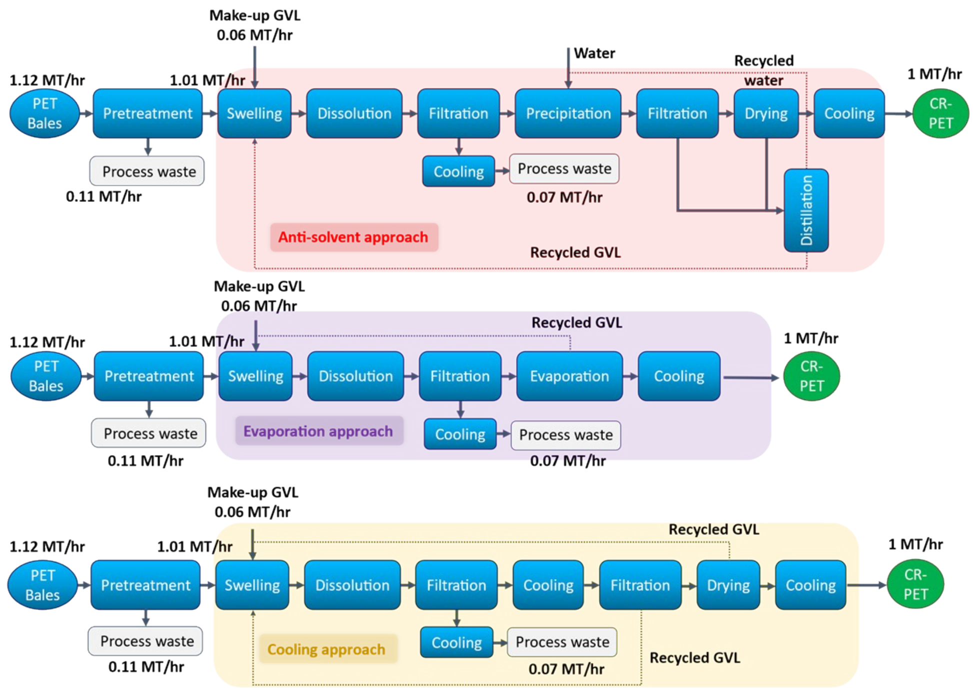

Fig. S1. Input and output material balance for all the simulated processes.

The process flow diagram and material balance for heat integrated PET dissolution process with precipitation via anti-solvent approach is shown in Fig. S2 and Table S4. The incoming process streams are stream no. 1 (PET flakes), 2, (make-up GVL), and 13 (water). The streams going out are stream no. 26 (CR-PET) and 12 (process loss).

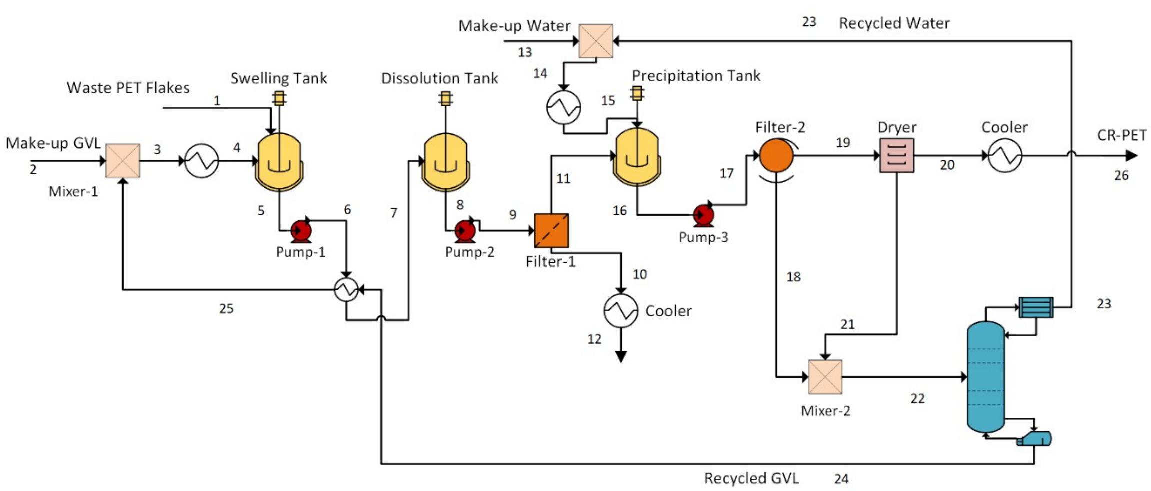

Fig. S2. Process flow diagram for heat integrated PET dissolution process with precipitation via anti-solvent approach.

Table S4. Material stream flows and compositions for heat integrated PET dissolution process with precipitation via anti-solvent approach.

Stream no.	1	2	3	4	5	6	7	8	9

Temp. (ºC)	25	25	146.99	138	120.69	120.69	170	170	170
Pressure (atm)	1	1	1	1	1	1	1	1	1
PET (kg/hr)	1010	0	0	0	1010	1010	1010	1010	1010
GVL (kg/hr)	0	60.01	4000.23	4000.23	4000.23	4000.23	4000.23	4000.23	4000.23
Water (kg/hr)	0	0	0.26	0.26	0.26	0.26	0.26	0.26	0.26
Stream no.	10	11	12	13	14	15	16	17	18
Temp. (ºC)	170	170	35	25	99.65	35	35	35	35
Pressure (atm)	1	1	1	1	1	1	1	1	1
PET (kg/hr)	9.99	1000	9.99	0	0	0	1000	1000	0
GVL (kg/hr)	60	3940.23	60	0	6.29	6.29	3946.52	3946.52	3663.25
Water (kg/hr)	0	0.26	0	0	4003.99	4003.99	4004.25	4004.25	3716.83
Stream no.	19	20	21	22	23	24	25	26	
Temp. (ºC)	35	207	207	77.04	99.98	207	148.69	25	
Pressure (atm)	1	1	1	1	1	1	1	1	
PET (kg/hr)	1000	1000	0	0	0	0	0	1000	
GVL (kg/hr)	283.27	0	283.27	3946.52	6.29	3940.23	3940.23	0	
Water (kg/hr)	287.42	0	287.42	4004.25	4003.99	0.26	0.26	0	

The process flow diagram and material balance for heat integrated PET dissolution process with precipitation via evaporation approach is shown in Fig. S3 and Table S5.

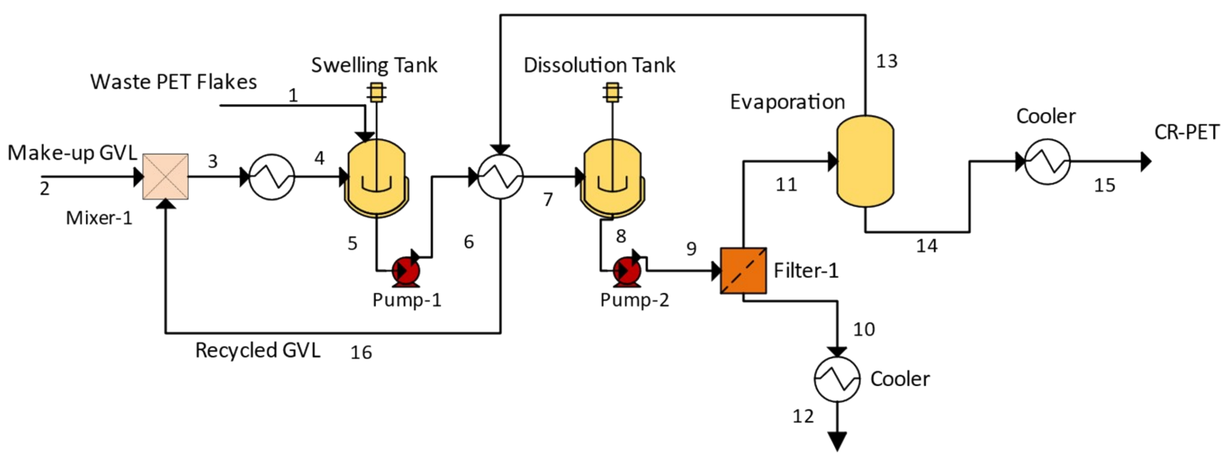

Fig. S3. Process flow diagram for heat integrated PET dissolution process with precipitation via evaporation approach.

Table S5. Material stream flows and compositions for heat integrated PET dissolution process with precipitation via evaporation approach.

Stream no.	1	2	3	4	5	6	7	8	9
Temp. (ºC)	25	25	207.41	138	120.69	120.69	170	170	170
Pressure (atm)	1	1	1	1	1	1	1	1	1

PET (kg/hr)	1010	0	0	0	1010	1010	1010	1010	1010
GVL (kg/hr)	0	60	3999.82	3999.82	3999.82	3999.82	3999.82	3999.82	3999.82
Stream no.	10	11	12	13	14	15	16		
Temp. (ºC)	170	170	35	207.42	207.42	35	207.41		
Pressure (atm)	1	1	1	1	1	1	1		
PET (kg/hr)	9.99	1000	9.99	0	1000	1000	0		
GVL (kg/hr)	60	3939.83	60	3939.83	0	0	3939.83		

The process flow diagram and material balance for PET dissolution process with precipitation via cooling approach is shown in Fig. S4 and Table S6.

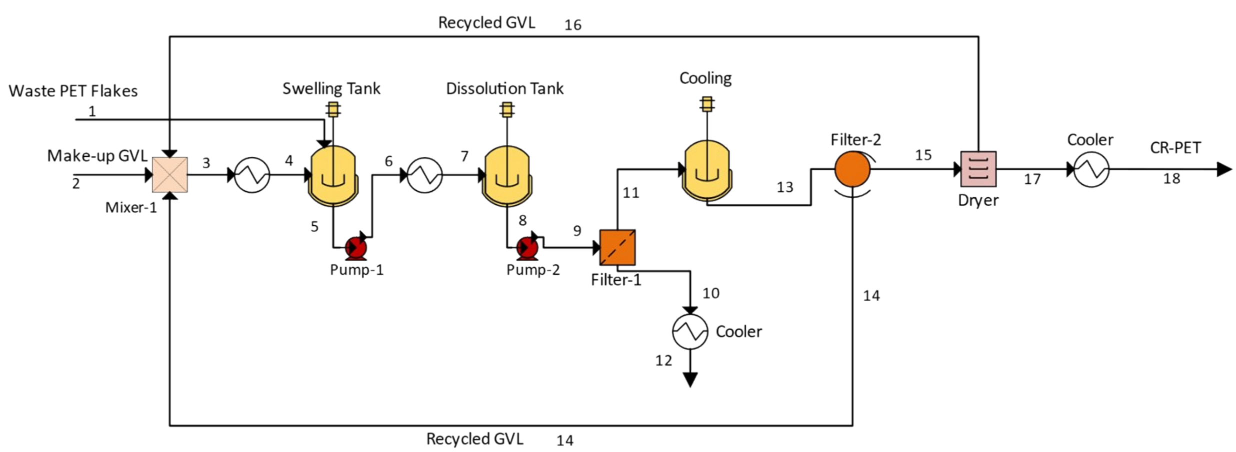

Fig. S4. Process flow diagram for PET dissolution process with precipitation via cooling approach.

Table S6. Material stream flows and compositions for PET dissolution process with precipitation via cooling approach.

Stream no.	1	2	3	4	5	6	7	8	9
Temp. (ºC)	25	25	96.29	138	120.69	120.69	170	170	170
Pressure (atm)	1	1	1	1	1	1	1	1	1

PET (kg/hr)	1010	0	0	0	1010	1010	1010	1010	1010
GVL (kg/hr)	0	60	3999.33	3999.33	3999.33	3999.33	3999.33	3999.33	3999.33
Stream no.	10	11	12	13	14	15	16	17	18
Temp. (ºC)	170	170	35	35	35	35	207.42	207.42	35
Pressure (atm)	1	1	1	1	1	1	1	1	1
PET (kg/hr)	9.99	1000	9.99	1000	0	1000	0	1000	1000
GVL (kg/hr)	60	3939.38	60	3939.38	3355.43	583.96	583.96	0	0

Table S7 shows the heating and cooling duties for all of the modeled process simulations. These heating and cooling duties served as an input for the LCA model in SimaPro software. These inputs were converted to represent the functional unit considered for the LCA, as shown in Table S3.

Table S7. Heating and cooling duties for modeled processes representing a production capacity of 8,400 MT/year (or 1 MT/hour).

	Anti-solvent		**Evaporation**		**Cooling**
	Base Case	**HIX**	**Base Case**	**HIX**	
Heating duty (GJ/hour)	25.96	25.45	2.66	2.15	1.60
% Savings	-2%		-19%		-
Cooling duty (GJ/hour)	25.63	25.12	2.34	1.83	1.28
% Savings	-2%		-22%		-

The discounted cash flow tables for all processes are shown in Table S8-S10 and the cumulative cash flow diagram is shown in Fig. S5 after these tables.

Table S8. Discounted cash flow table for heat integrated PET dissolution process with precipitation via anti-solvent approach.

Year	**Gross Profit ($MM)**	**Depreciation Charge ($MM)**	**Taxable Income ($MM)**	**Taxes Paid ($MM)**	**Cash Flow ($MM)**	**Discount Factor**	**Present Value of Cash Flow ($MM)**
-2					-0.89	1.44	-1.28
-1					-6.69	1.20	-8.03
0					-4.13	1.00	-4.13
1	2.11	1.59	0.52	0.11	2.00	0.83	1.67
2	4.03	2.73	1.30	0.27	3.76	0.69	2.61
3	4.03	1.95	2.08	0.44	3.60	0.58	2.08
4	4.03	1.39	2.64	0.55	3.48	0.48	1.68
5	4.03	1.00	3.04	0.64	3.40	0.40	1.36

6	4.03	0.99	3.04	0.64	3.40	0.33	1.14
7	4.03	1.00	3.04	0.64	3.40	0.28	0.95
8	4.03	0.50	3.54	0.74	3.29	0.23	0.77
9	4.03	-	4.03	0.85	3.19	0.19	0.62
10	4.03	-	4.03	0.85	3.19	0.16	0.51
11	4.03	-	4.03	0.85	3.19	0.13	0.43
12	4.03	-	4.03	0.85	3.19	0.11	0.36
13	4.03	-	4.03	0.85	3.19	0.09	0.30
14	4.03	-	4.03	0.85	3.19	0.08	0.25
15	4.03	-	4.03	0.85	3.19	0.06	0.21
16	4.03	-	4.03	0.85	3.19	0.05	0.17
17	4.03	-	4.03	0.85	3.19	0.05	0.14
18	4.03	-	4.03	0.85	3.19	0.04	0.12
19	4.03	-	4.03	0.85	3.19	0.03	0.10
20	4.03	-	4.03	0.85	3.19	0.03	0.08
21	4.03	-	4.03	0.85	3.19	0.02	0.07
22	4.03	-	4.03	0.85	3.19	0.02	0.06
23	4.03	-	4.03	0.85	3.19	0.02	0.05
24	4.03	-	4.03	0.85	3.19	0.01	0.04
25	4.03	-	4.03	0.85	3.19	0.01	0.03
26	4.03	-	4.03	0.85	3.19	0.01	0.03
27	4.03	-	4.03	0.85	3.19	0.01	0.02
28	4.03	-	4.03	0.85	3.19	0.01	0.02
29	4.03	-	4.03	0.85	3.19	0.01	0.02
30	4.03	-	4.03	0.85	2.63	0.00	0.01
NPV ($ MM)							**2.45**

Table S9. Discounted cash flow table for heat integrated PET dissolution process with precipitation via evaporation approach.

Year	Gross Profit ($MM)	Depreciation Charge ($MM)	Taxable Income ($MM)	Taxes Paid ($MM)	Cash Flow ($MM)	Discount Factor	Present Value of Cash Flow ($MM)
-2					-0.68	1.44	-0.97
-1					-5.07	1.20	-6.08
0					-3.13	1.00	-3.13
1	3.34	1.21	2.13	0.45	2.89	0.83	2.41
2	5.42	2.07	3.35	0.70	4.72	0.69	3.28
3	5.42	1.48	3.95	0.83	4.59	0.58	2.66
4	5.42	1.06	4.37	0.92	4.51	0.48	2.17
5	5.42	0.75	4.67	0.98	4.44	0.40	1.79
6	5.42	0.75	4.67	0.98	4.44	0.33	1.49

7	5.42	0.75	4.67	0.98	4.44	0.28	1.24
8	5.42	0.38	5.05	1.06	4.36	0.23	1.01
9	5.42	-	5.42	1.14	4.28	0.19	0.83
10	5.42	-	5.42	1.14	4.28	0.16	0.69
11	5.42	-	5.42	1.14	4.28	0.13	0.58
12	5.42	-	5.42	1.14	4.28	0.11	0.48
13	5.42	-	5.42	1.14	4.28	0.09	0.40
14	5.42	-	5.42	1.14	4.28	0.08	0.33
15	5.42	-	5.42	1.14	4.28	0.06	0.28
16	5.42	-	5.42	1.14	4.28	0.05	0.23
17	5.42	-	5.42	1.14	4.28	0.05	0.19
18	5.42	-	5.42	1.14	4.28	0.04	0.16
19	5.42	-	5.42	1.14	4.28	0.03	0.13
20	5.42	-	5.42	1.14	4.28	0.03	0.11
21	5.42	-	5.42	1.14	4.28	0.02	0.09
22	5.42	-	5.42	1.14	4.28	0.02	0.08
23	5.42	-	5.42	1.14	4.28	0.02	0.06
24	5.42	-	5.42	1.14	4.28	0.01	0.05
25	5.42	-	5.42	1.14	4.28	0.01	0.04
26	5.42	-	5.42	1.14	4.28	0.01	0.04
27	5.42	-	5.42	1.14	4.28	0.01	0.03
28	5.42	-	5.42	1.14	4.28	0.01	0.03
29	5.42	-	5.42	1.14	4.28	0.01	0.02
30	5.42	-	5.42	1.14	3.86	0.00	0.02
NPV ($ MM)							**10.75**

Table S10. Discounted cash flow table for PET dissolution process with precipitation via cooling approach.

Year	Gross Profit ($MM)	Depreciation Charge ($MM)	Taxable Income ($MM)	Taxes Paid ($MM)	Cash Flow ($MM)	Discount Factor	Present Value of Cash Flow ($MM)
-2					-0.83	1.44	-1.19
-1					-6.19	1.20	-7.43
0					-3.82	1.00	-3.82
1	3.33	1.47	1.86	0.39	2.94	0.83	2.45
2	5.43	2.53	2.90	0.61	4.82	0.69	3.35
3	5.43	1.81	3.62	0.76	4.67	0.58	2.70
4	5.43	1.29	4.14	0.87	4.56	0.48	2.20
5	5.43	0.92	4.50	0.95	4.48	0.40	1.80
6	5.43	0.92	4.50	0.95	4.48	0.33	1.50
7	5.43	0.92	4.50	0.95	4.48	0.28	1.25

8	5.43	0.46	4.97	1.04	4.38	0.23	1.02
9	5.43	-	5.43	1.14	4.29	0.19	0.83
10	5.43	-	5.43	1.14	4.29	0.16	0.69
11	5.43	-	5.43	1.14	4.29	0.13	0.58
12	5.43	-	5.43	1.14	4.29	0.11	0.48
13	5.43	-	5.43	1.14	4.29	0.09	0.40
14	5.43	-	5.43	1.14	4.29	0.08	0.33
15	5.43	-	5.43	1.14	4.29	0.06	0.28
16	5.43	-	5.43	1.14	4.29	0.05	0.23
17	5.43	-	5.43	1.14	4.29	0.05	0.19
18	5.43	-	5.43	1.14	4.29	0.04	0.16
19	5.43	-	5.43	1.14	4.29	0.03	0.13
20	5.43	-	5.43	1.14	4.29	0.03	0.11
21	5.43	-	5.43	1.14	4.29	0.02	0.09
22	5.43	-	5.43	1.14	4.29	0.02	0.08
23	5.43	-	5.43	1.14	4.29	0.02	0.06
24	5.43	-	5.43	1.14	4.29	0.01	0.05
25	5.43	-	5.43	1.14	4.29	0.01	0.04
26	5.43	-	5.43	1.14	4.29	0.01	0.04
27	5.43	-	5.43	1.14	4.29	0.01	0.03
28	5.43	-	5.43	1.14	4.29	0.01	0.03
29	5.43	-	5.43	1.14	4.29	0.01	0.02
30	5.43	-	5.43	1.14	3.77	0.00	0.02
NPV ($ MM)							**8.72**

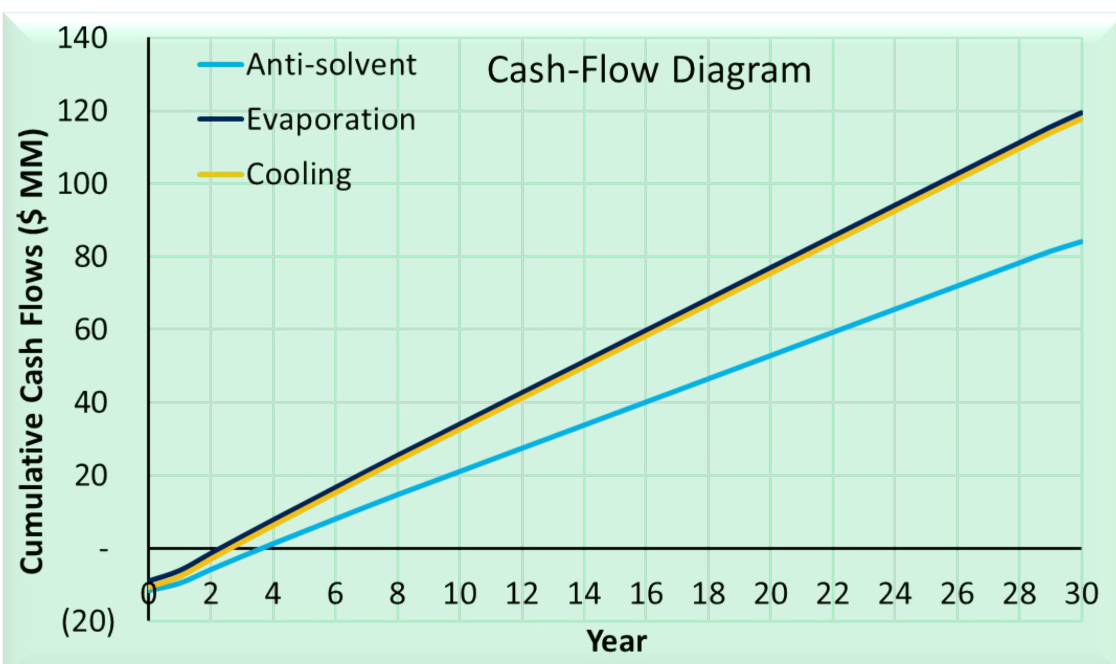

Fig. S5. Cumulative cash flow diagram for all modeled processes. Note: The point at which the cumulative cash flow curve intersects the X-axis represents the payback period.

Table S11 shows variable and fixed operating costs in $MM/year for modeled processes at a capacity of 8,400 MT/year.

Table S11. Fixed and variable operating costs for economic analysis of waste PET dissolution processes at base capacity.

Costs ($ MM/Year)	Anti-solvent		Evaporation		Cooling
	Base Case	HIX	Base Case	HIX	
Feedstock	3.56				
Bale pretreatment	0.94				
Utilities	1.47	1.46	0.16	0.14	0.087
Raw material	0.50				
Waste treatment	0.08				
Transportation costs	0.07				
Fixed operating costs	2.87	2.87	2.8	0.8	2.85

Fig. S6 shows the transportation costs in $/MT and in $/year along with unit delivery cost as a function of capacity.

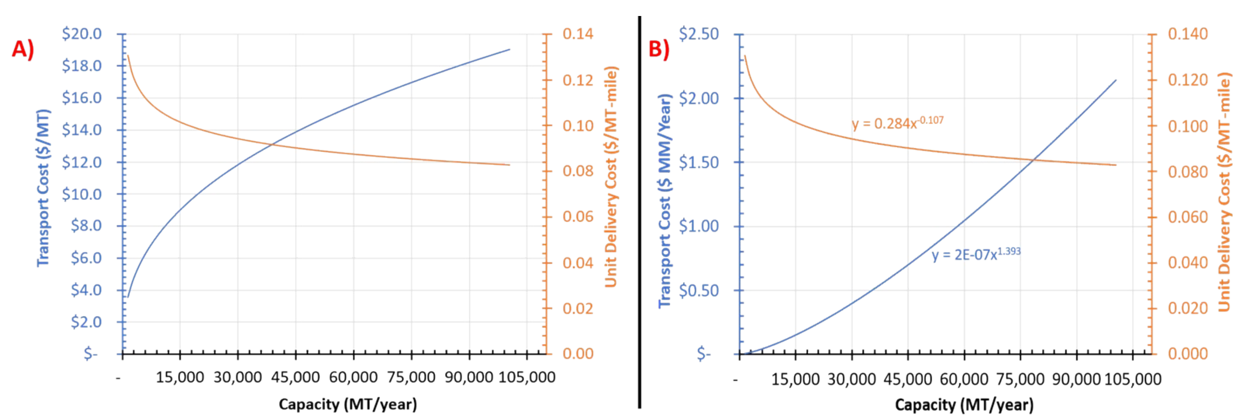

Fig. S6. Transportation costs and unit delivery costs as a function of capacity. A) Transportation costs ($/MT) B) Transportation costs ($MM/year)

The total costs of production for modeled processes are shown in Fig. S7. It was determined by adding operating costs and annualized capital costs (ACC), as described by Towler et al.[48]. The ACC was determined to be 0.201 for the assumed interest rate (‘i’) of 20% for the total project life period of 30 years (‘n’). Feedstock costs, fixed operating costs, and capital costs dominated the cost of production at 8,400 MT/year of capacity. The total costs of production decrease with increasing production capacity as shown in Fig. 5 of the main manuscript.

$$Total\ cost\ of\ production = Operating\ costs + ACC$$

$$Annual\ Capital\ Cost\ (ACC) = Annual\ Capital\ Cost\ Ratio\ (ACCR) \times Total\ FCI$$

$$ACCR = \frac{[i\,(1+i)^n]}{[(1+i)^n - 1]}$$

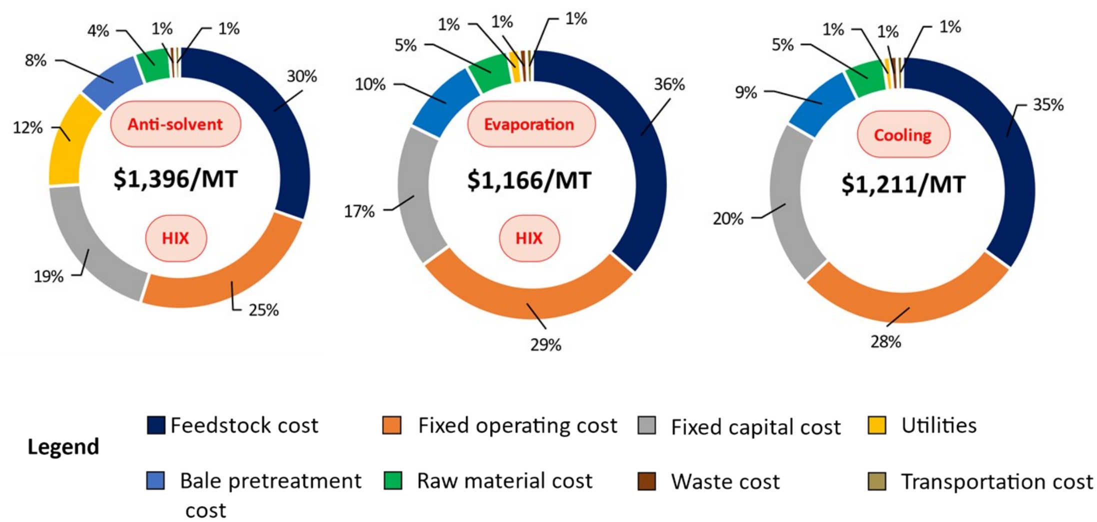

Fig. S7. Total cost of production per metric ton of CR-PET produced. Notes: 1) Results shown for the base capacity. 2) HIX refers to heat integrated process.

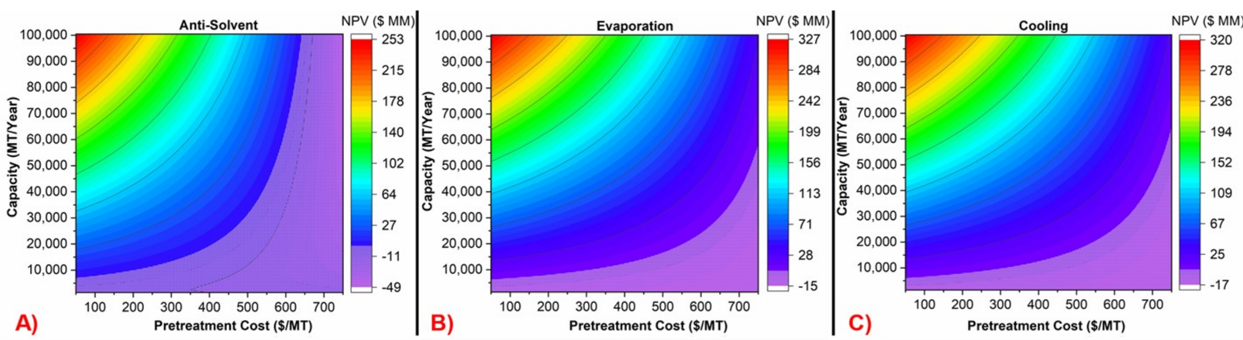

Fig. S8. NPV as a function of capacity and pretreatment costs for the modeled processes. Note: This analysis was conducted at a constant feedstock cost of $377/MT. The NPV=0 line is at the interface between the purple and blue colors. This interface represents the minimum capacity to achieve profitability.

Fig. S9 shows the environmental impacts associated with only transportation as a function of capacity. These impacts represent average GHG emissions and CED associated with transportation of the baled PET feedstock, as described in section 3 of this document.

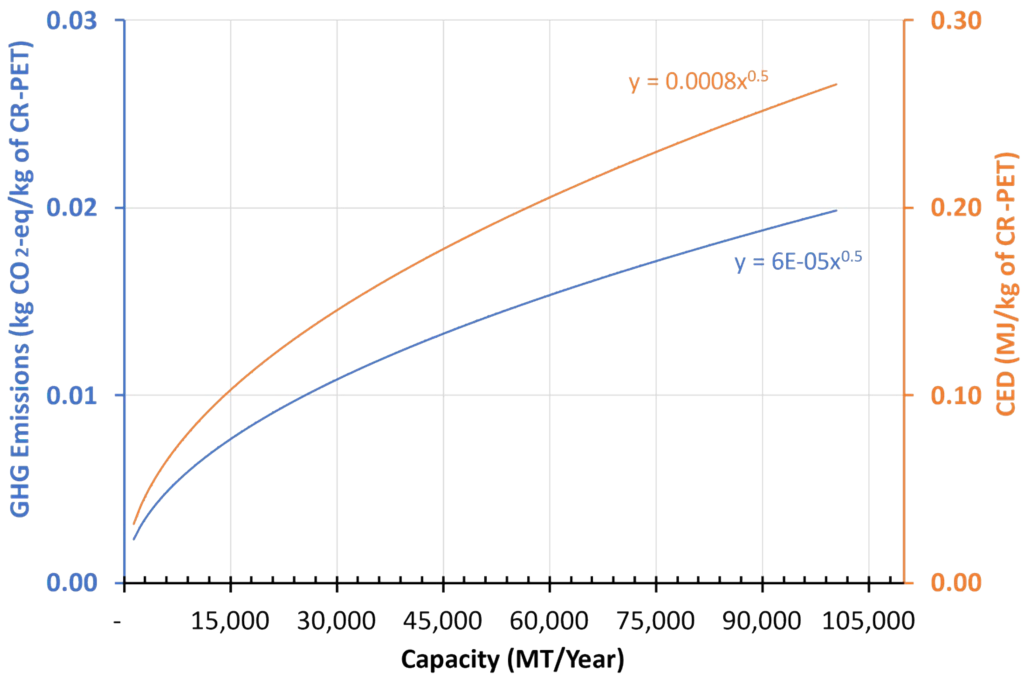

Fig. S9. Transportation related GHG emissions and total energy demand as function of capacity. Note: Mode of transportation was assumed to be via truck only.

References

1. Closed Loop Partners, Accelerating circular supply chains for plastics: A landscape of transformational technologies that stop plastic waste keep materials in play and grow markets, https://www.closedlooppartners.com/wp-content/uploads/2020/01/CLP_Circular_Supply_Chains_for_Plastics.pdf, (accessed November 23, 2020).
2. J.-P. Lange, *ACS Sustainable Chemistry Engineering*, 2021, **9**, 15722-15738.
3. A. del Carmen Munguía-López, D. Göreke, K. L. Sánchez-Rivera, H. A. Aguirre-Villegas, S. Avraamidou, G. W. Huber and V. M. Zavala, *Green Chemistry*, 2023, **25**, 1611-1625.
4. K. L. Sánchez-Rivera, P. Zhou, M. S. Kim, L. D. González Chávez, S. Grey, K. Nelson, S. C. Wang, I. Hermans, V. M. Zavala and R. C. Van Lehn, *ChemSusChem*, 2021, **14**, 4317-4329.
5. T. W. Walker, N. Frelka, Z. Shen, A. K. Chew, J. Banick, S. Grey, M. S. Kim, J. A. Dumesic, R. C. Van Lehn and G. W. Huber, *Science advances*, 2020, **6**, eaba7599.
6. T. Uekert, A. Singh, J. S. DesVeaux, T. Ghosh, A. Bhatt, G. Yadav, S. Afzal, J. Walzberg, K. M. Knauer and S. R. Nicholson, *ACS Sustainable Chemistry Engineering*, 2023.
7. U. S. Chaudhari, D. G. Kulas, A. Peralta, T. Hossain, A. T. Johnson, D. S. Hartley, R. M. Handler, B. K. Reck, V. S. Thompson, D. Watkins and D. R. Shonnard, Washington DC, 2023.
8. U. R. Gracida-Alvarez, O. Winjobi, J. C. Sacramento-Rivero and D. R. Shonnard, *ACS Sustainable Chemistry & Engineering*, 2019, **7**, 18254-18266.
9. U. R. Gracida-Alvarez, O. Winjobi, J. C. Sacramento-Rivero and D. R. Shonnard, *ACS Sustainable Chemistry & Engineering*, 2019, **7**, 18267-18278.
10. D. G. Kulas, A. Zolghadr, U. S. Chaudhari and D. R. Shonnard, *Journal of Cleaner Production*, 2023, **384**, 135542.
11. R. R. Bora, R. Wang and F. You, *ACS Sustainable Chemistry & Engineering*, 2020, **8**, 16350-16363.
12. G. Yadav, A. Singh, A. Dutta, T. Uekert, J. DesVeaux, S. R. Nicholson, E. C. Tan, C. Mukarakate, J. A. Schaidle and C. Wrasman, *Energy & Environmental Science*, 2023.
13. G. Jiang, J. Wang, S. M. Al-Salem and G. A. Leeke, *Energy & Fuels*, 2020, **34**, 7397-7409.
14. S. H. Zein, C. T. Grogan, O. Y. Yansaneh and A. Putranto, *Processes*, 2022, **10**, 1503.
15. C. Lubongo, T. Congdon, J. McWhinnie and P. Alexandridis, *Sustainable Chemistry and Pharmacy*, 2022, **27**, 100683.
16. P. T. Benavides, P. Sun, J. Han, J. B. Dunn and M. Wang, *Fuel*, 2017, **203**, 11-22.
17. A. Fivga and I. Dimitriou, *Energy*, 2018, **149**, 865-874.
18. M. Larrain, S. Van Passel, G. Thomassen, U. Kresovic, N. Alderweireldt, E. Moerman and P. Billen, *Journal of Cleaner Production*, 2020, **270**, 122442.
19. F. Riedewald, Y. Patel, E. Wilson, S. Santos and M. Sousa-Gallagher, *Waste Management*, 2021, **120**, 698-707.
20. H. Jeswani, C. Krüger, M. Russ, M. Horlacher, F. Antony, S. Hann and A. Azapagic, *Science of the Total Environment*, 2021, **769**, 144483.
21. S. Das, C. Liang and J. B. Dunn, *Waste Management*, 2022, **153**, 81-88.
22. A. d. R. D. Monteiro, D. M. V. de Miranda, J. C. C. da Silva Pinto and J. J. Soto, *Macromolecular Reaction Engineering*, 2022, **16**, 2200037.
23. S. Afzal, A. Singh, S. R. Nicholson, T. Uekert, J. DesVeaux, E. C. Tan, A. Dutta, A. Carpenter, R. Baldwin and G. T. Beckham, *Green Chemistry*, 2023.

24. D. Cudjoe and H. Wang, *Fuel Processing Technology*, 2022, **237**, 107470.
25. K. Lan and Y. Yao, *Communications Earth & Environment*, 2022, **3**, 300.
26. A. Schwarz, T. Ligthart, D. G. Bizarro, P. De Wild, B. Vreugdenhil and T. Van Harmelen, *Waste Management*, 2021, **121**, 331-342.
27. M. K. van der Hulst, A. B. Ottenbros, B. van der Drift, Š. Ferjan, T. van Harmelen, A. E. Schwarz, E. Worrell, R. van Zelm, M. A. Huijbregts and M. Hauck, *Resources, Conservation and Recycling*, 2022, **186**, 106582.
28. V. Cappello, P. Sun, G. Zang, S. Kumar, R. Hackler, H. E. Delgado, A. Elgowainy, M. Delferro and T. Krause, *Green Chemistry*, 2022, **24**, 6306-6318.
29. M. C. Ozoemena and S. R. Coles, *Journal of Polymers and the Environment*, 2023, 1-11.
30. F. Keller, R. L. Voss, R. P. Lee and B. Meyer, *Resources, Conservation and Recycling*, 2022, **179**, 106106.
31. R. Voss, R. P. Lee and M. Fröhling, *Circular Economy and Sustainability*, 2022, **2**, 1369-1398.
32. R. Voss, R. P. Lee and M. Fröhling, *Journal of Industrial Ecology*, 2022.
33. S. Zallaya, J. H. El Achkar, A. Abou Chacra, S. Shatila, J. El Akhdar and Y. Daher, *Chemical Engineering Science*, 2023, **267**, 118340.
34. P. Naviroj, J. Treacy and C. Urffer, 2019.
35. K. Phan, S. Ügdüler, L. Harinck, R. Denolf, M. Roosen, G. O'Rourke, D. De Vos, V. Van Speybroeck, K. De Clerck and S. De Meester, *Resources, Conservation and Recycling*, 2023, **191**, 106903.
36. A. Singh, N. A. Rorrer, S. R. Nicholson, E. Erickson, J. S. DesVeaux, A. F. Avelino, P. Lamers, A. Bhatt, Y. Zhang and G. Avery, *Joule*, 2021, **5**, 2479-2503.
37. Benard Nyawanga, Master of Science, University of South Florida, 2021.
38. S. Cornago, D. Rovelli, C. Brondi, M. Crippa, B. Morico, A. Ballarino and G. Dotelli, *Journal of Cleaner Production*, 2021, **311**, 127406.
39. T. Uekert, J. S. DesVeaux, A. Singh, S. R. Nicholson, P. Lamers, T. Ghosh, J. E. McGeehan, A. C. Carpenter and G. T. Beckham, *Green Chemistry*, 2022, **24**, 6531-6543.
40. S. Ügdüler, K. M. Van Geem, R. Denolf, M. Roosen, N. Mys, K. Ragaert and S. De Meester, *Green chemistry*, 2020, **22**, 5376-5394.
41. U. R. Gracida-Alvarez, H. Xu, P. T. Benavides, M. Wang and T. R. Hawkins, *ACS Sustainable Chemistry & Engineering*, 2023, **11**, 514-524.
42. S. Yousef, J. Eimontas, I. Stasiulaitiene, K. Zakarauskas and N. Striūgas, *Sustainable production and consumption*, 2022, **32**, 519-531.
43. X. Zhao, J. J. Klemeš and F. You, *Renewable and Sustainable Energy Reviews*, 2022, **153**, 111786.
44. X. Zhao and F. You, *ACS Sustainable Chemistry & Engineering*, 2021, **9**, 12167-12184.
45. B. Hernández, P. Kots, E. Selvam, D. G. Vlachos and M. G. Ierapetritou, *ACS Sustainable Chemistry & Engineering*, 2023, **11**, 7170-7181.
46. J. Yu, A. del Carmen Munguía-López, V. S. Cecon, K. L. Sánchez-Rivera, K. Nelson, J. Wu, S. Kolapkar, V. M. Zavala, G. W. Curtzwiler and K. L. Vorst, *Green Chemistry*, 2023, **25**, 4723-4734.
47. K. L. Sánchez-Rivera, A. del Carmen Munguía-López, P. Zhou, V. S. Cecon, J. Yu, K. Nelson, D. Miller, S. Grey, Z. Xu and E. Bar-Ziv, *Resources, Conservation and Recycling*, 2023, **197**, 107086.

48. G. Towler and R. Sinnott, *Chemical engineering design: principles, practice and economics of plant and process design*, Butterworth-Heinemann, 2021.
49. A. Dutta, A. Sahir, E. Tan, D. Humbird, L. J. Snowden-Swan, P. A. Meyer, J. Ross, D. Sexton, R. Yap and J. Lukas, *Process design and economics for the conversion of lignocellulosic biomass to hydrocarbon fuels: Thermochemical research pathways with in situ and ex situ upgrading of fast pyrolysis vapors*, Pacific Northwest National Lab.(PNNL), Richland, WA (United States), 2015.
50. Resource Recycling Systems (RRS), https://recycle.com/, (accessed July 4, 2023).
51. D. M. Alonso, S. H. Hakim, S. Zhou, W. Won, O. Hosseinaei, J. Tao, V. Garcia-Negron, A. H. Motagamwala, M. A. Mellmer and K. Huang, *Science advances*, 2017, **3**, e1603301.
52. Environmental Research & Education Foundation, Analysis of MSW Landfill Tipping Fees: 2021, https://erefdn.org/product/analysis-of-msw-landfill-tipping-fees-2021-pdf/, (accessed July 4, 2023).
53. U.S. Energy Information Administration (EIA), Electric Power Annual: Table 2.4 Average Price of Electricity to Ultimate Customers, https://www.eia.gov/electricity/annual/, (accessed July 4, 2023).
54. R. C. B. Richard Turton, Wallace B. Whiting, Joseph A. Shaeiwitz, Debangsu Bhattacharya, Analysis Synthesis and Design of Chemical Processes 5th Edition, https://richardturton.faculty.wvu.edu/publications/analysis-synthesis-and-design-of-chemical-processes-5th-edition, (accessed July 4, 2023).
55. U.S. Energy Information Administration (EIA), United States Natural Gas Industrial Price, https://www.eia.gov/dnav/ng/hist/n3035us3A.htm, (accessed July 4, 2023).
56. M. Wright and R. C. Brown, *Biofuels, Bioproducts and Biorefining: Innovation for a sustainable economy*, 2007, **1**, 191-200.
57. M. M. Wright, R. C. Brown and A. A. Boateng, *Biofuels, bioproducts and biorefining*, 2008, **2**, 229-238.
58. B. M. Jenkins, *Biomass and bioenergy*, 1997, **13**, 1-9.
59. T. Hossain, D. Jones, D. Hartley, L. M. Griffel, Y. Lin, P. Burli, D. N. Thompson, M. Langholtz, M. Davis and C. Brandt, *Applied Energy*, 2021, **294**, 116946.
60. United States Census Bureau, Quick Facts: United States, https://www.census.gov/quickfacts/fact/table/US/POP060220#POP060220, (accessed July 4, 2023).
61. U.S. EPA, Advancing Sustainable Materials Management: 2018 Tables and Figures Report, https://www.epa.gov/facts-and-figures-about-materials-waste-and-recycling/advancing-sustainable-materials-management, (accessed July 4, 2023).
62. United States Census Bureau, Urban and Rural, https://www.census.gov/programs-surveys/geography/guidance/geo-areas/urban-rural.html, (accessed July 4, 2023).
63. United States Census Bureau, 2020 Census Urban Areas Facts, https://www.census.gov/programs-surveys/geography/guidance/geo-areas/urban-rural/2020-ua-facts.html, (accessed July 4, 2023).
64. Ecoinvent, Ecoinvent database for transport sector - Freight transport, https://ecoinvent.org/the-ecoinvent-database/sectors/transport/#1592220812641-df7fe628-a0f21598366392497161457800423616316318856 43, (accessed July 6, 2023).
65. M. Otten, STREAM Freight Transport 2020-Emissions of freight transport modes, https://cedelft.eu/publications/stream-freight-transport-2020/, (accessed July 6, 2023).

66. Franklin Associates, Life cycle impacts for postconsumer recycled resins: PET, HDPE, and PP, https://plasticsrecycling.org/images/apr/2018-APR-Recycled-Resin-Report.pdf, (accessed April 23, 2022).